

Na⁺/Ca²⁺ Exchanger 2 in the Circadian Clock of the Rat Suprachiasmatic Nucleus: Colocalization with Neuropeptides and Daily Profiles of Gene Expression and Protein Levels

Pi-Cheng Cheng¹, Ya-Shuan Chen¹, and Rong-Chi Huang^{1, 2, 3}

¹Department of Physiology and Pharmacology, College of Medicine, Chang Gung University

²Healthy Aging Research Center, Chang Gung University

and

³Neuroscience Research Center, Chang Gung Memorial Hospital, Linkou Medical Center, Tao-Yuan 33305, Taiwan, Republic of China

Abstract

The plasmalemmal Na⁺/Ca²⁺ exchanger (NCX) regulates intracellular Ca²⁺ by exchanging 3 Na⁺ for 1 Ca²⁺ in either the Ca²⁺ exit or Ca²⁺ entry mode. All three NCX isoforms NCX1, NCX2, and NCX3 are expressed in the rat brain, with isoform-specific differential distribution. In the central clock of suprachiasmatic nucleus (SCN), intracellular Ca²⁺ controls the circadian release of major neuropeptides, which are the arginine vasopressin (AVP), vasoactive intestinal peptide (VIP) and gastrin releasing peptide (GRP), and the NCX, most likely NCX1, rapidly clears depolarization-induced somatic Ca²⁺ influx. However, the role of NCX2 in the SCN remains unknown. This study aimed to investigate the colocalization of NCX2 with neuropeptides and daily expression profiles of NCX2 in mRNA and protein levels. Consistent with the restricted distribution of NCX2 in the retinorecipient ventral SCN, the immunostaining results showed colocalization of NCX2 with VIP, GRP and VIP/GRP in the ventral SCN, but not with AVP in the dorsal SCN, or markers for astrocyte and major input pathways. Importantly, the presynaptic marker Bassoon was found to colocalize with NCX2/GRP and NCX2/VIP, indicating localization of both VIP/NCX2 and GRP/NCX2 at the presynaptic sites. Furthermore, real-time polymerase chain reaction (PCR) and western blotting revealed no day-night difference in NCX2 mRNA and protein levels, in contrast to a robust circadian rhythm in the expression of clock genes *Per1* and *Per2*. Together the results suggest a role of NCX2 in the regulation of the release of VIP and GRP.

Key Words: arginine vasopressin, Bassoon, Ca²⁺, circadian rhythm, gastrin releasing peptide, Na⁺/Ca²⁺ exchanger, suprachiasmatic nucleus, vasoactive intestinal peptide

Introduction

The plasmalemmal Na⁺/Ca²⁺ exchanger (NCX) exchanges 3 Na⁺ for 1 Ca²⁺ in either the Ca²⁺ exit or the Ca²⁺ entry mode (4). Under physiological conditions, an increase in [Ca²⁺]_i would activate the Ca²⁺ exit mode to extrude Ca²⁺, and an increase in [Na⁺]_i could activate the Ca²⁺ entry mode to uptake Ca²⁺. As

such, NCX plays an important role in the regulation of intracellular Ca²⁺ homeostasis. There are three NCX isoforms, NCX1, NCX2, and NCX3 (25, 35, 36), all of which are found to be expressed in the rat brain (24, 38, 46). All three isoforms have similar properties (17, 26), but the isoform-specific distribution in different brain regions, cell types and subcellular localization (38, 43; for review see ref. 40) suggests

distinct functions for different isoforms. For examples, knockouts of NCX specific isoforms have revealed differential roles of NCX2 and NCX3 in the regulation of presynaptic and postsynaptic $[Ca^{2+}]_i$ in the mouse CA1 hippocampal neurons (18, 31).

The hypothalamic suprachiasmatic nucleus (SCN) is the central clock that controls circadian rhythms in mammals (9). The SCN clock can be entrained by both photic and non-photoc inputs to synchronize daily activities. In rats, photic information from the retina is transmitted by the glutamatergic retino-hypothalamic tract to reach and entrain the gastrin releasing peptide (GRP)- and vasoactive intestinal peptide (VIP)-positive ventral “core” SCN (16, 30), which then innervates and entrains the arginine vasopressin (AVP)-positive dorsal “shell” SCN (23). As such, both VIP and GRP are important in transducing photic information and are also critical for proper functioning of the SCN clock (5, 28). Non-photoc cues entrain the SCN clock *via* serotonergic projections from the median raphe nucleus and *via* projections of neuropeptide Y (NPY) from the intergeniculate leaflet, with both pathways also targeting the ventral SCN (for review, see ref. 33). *In vivo* microdialysis experiments have demonstrated a Ca^{2+} -dependent circadian release of AVP, VIP and GRP from the hamster SCN (13, 14). To investigate the regulation of Ca^{2+} homeostasis in the SCN neurons, we recently showed that the SCN expressed NCX1 and NCX2, with NCX1 distributed in the whole SCN, but NCX2 distribution was restricted to the ventral SCN, a region corresponding to the VIP- and GRP-positive area that receives major afferent inputs (44). Importantly, NCX, most likely NCX1, was also shown to play an important role in the rapid clearance of depolarization-induced Ca^{2+} influx in neurons from both dorsal and ventral SCN (44) However, the role of NCX2 in the SCN remains unknown.

This study aimed to investigate the colocalization of NCX2 with neuropeptides and daily expression profiles of NCX2 in mRNA and protein levels. Well-characterized antibodies against NCX2, AVP, VIP, and GRP were used to investigate the distribution patterns of these antigens. Double and triple staining immunofluorescence was performed to determine the localization of NCX2 with the three major peptides and with the presynaptic marker protein Bassoon. Furthermore, real-time polymerase chain reaction (PCR) and western blotting were used to quantify the expression of mRNA and protein levels of NCX2 at different time points throughout the day. Our results indicated selective localization of NCX2 with VIP, GRP, and VIP/GRP, as well as the presence of triple stains for both Bassoon/NCX2/VIP and Bassoon/NCX2/GRP. Nevertheless, there was no day-night

difference in NCX2 mRNA and protein levels. Together, the results suggest that NCX2 plays a role in the regulation of release of VIP and GRP.

Materials and Methods

Hypothalamic Brain Slices and SCN Isolation

All experiments were carried out according to procedures approved by the Institutional Animal Care and Use Committee of Chang Gung University. Sprague-Dawley rats (20–24 days old) were kept in a temperature-controlled room under a 12:12 light:dark cycle (light on 0700–1900 h). Lights-on was designated as Zeitgeber time (ZT) 0. An animal of either sex was carefully restrained by hand to reduce stress and killed by quick decapitation using a small rodent guillotine without anaesthesia, and the brain was put in an ice-cold artificial cerebrospinal fluid (ACSF) prebubbled with 95% O_2 mixed with 5% CO_2 . The ACSF contained 125 mM NaCl, 3.5 mM KCl, 2 mM $CaCl_2$, 1.5 mM $MgCl_2$, 26 mM $NaHCO_3$, 1.2 mM NaH_2PO_4 , 10 mM glucose. A 400 μ m coronal slice containing the SCN and the optic chiasm was cut with a DSK microslicer DTK-1000 (Ted Pella, Redding, CA, USA), and was then incubated at room temperature at 22–25°C in the incubation solution, which contained 140 mM NaCl, 3.5 mM KCl, 2 mM $CaCl_2$, 1.5 mM $MgCl_2$, 10 mM glucose, 10 mM HEPES, pH 7.4, bubbled with 100% O_2 . The SCN was isolated with a fine needle (cat no. 26002-10, Fine Science Tools, Foster City, CA, USA) under a dissecting microscope. For western blotting, the isolated SCN was frozen on dry ice and then maintained at –80°C until analysis.

RNA Extraction and cDNA Synthesis

Total mRNA of the SCN was prepared from freshly dissected tissues by extraction with the Absolutely RNA Nanoprep kit (Stratagene, La Jolla, CA, USA) according to the manufacturer's instructions. The purity of the total RNA in each sample was measured using a microplate spectrophotometer reader (Multiskan GO; Thermo Fisher Scientific, Waltham, MA, USA). Samples were volume-adjusted with RNAase-free water and normalized for their RNA content. The resulting RNA was reverse-transcribed to cDNA with Superscript III reverse transcriptase (Invitrogen, Carlsbad, CA, USA) and the oligo(dT)_{12–18} primers in a total volume of 30 μ l.

Real-Time PCR Analysis of mRNA Levels of NCX2, Per1 and Per2

The mRNA expression levels of NCX2, Per1, and Per2 were measured by real-time PCR analysis

with the SYBR Green method. The target genes and *Glyceraldehyde 3-phosphate dehydrogenase (GAPDH)* were amplified separately using the same group of cDNA template from each sample. Successful reverse transcription was confirmed for all samples by performing PCR amplification of the internal control *GAPDH*. Primer sequences for target genes were as follows: *GAPDH*: forward 5'-TGATGCCCCA-TGTTTGTG-3' and reverse 5'-GCTGACAATCT-TGAGGGAGTTGT-3'; *Per1*: forward 5'-TGTGTG-GACTGTGGTAGC-3' and reverse 5'-TCTGAGAA-GAGAGGGTTCG-3'; *Per2*: forward 5'-CCAGAG-GCGAGAGCTTC-3' and reverse 5'-GATGGCG-GTAGGCAGAC-3'; *NCX2*: forward 5'-GCGTGTG-GGCGATGCTCA-3' and reverse 5'-GACCTCGAG-GCGACAGTTC-3'. PCR amplification was carried out using 2× Power SYBR Green PCR Master Mix (Applied Biosystems, Framingham, MA, USA) in the StepOne Real Time PCR System (48-well format) (Applied Biosystems). The PCR reaction setup included 10 μl 2× Power SYBR Green PCR Master Mix, 0.6 μl 10 μM forward primer, 0.6 μl 10 μM reverse primer and 2 μl (10 ng) cDNA in a total reaction volume of 20 μl. Cycle threshold (CT) values were obtained from the exponential phase of the PCR amplification. The $2^{-\Delta\Delta C_T}$ method was used to calculate the mRNA levels normalized to that of *GAPDH* ($\Delta C_T = \text{target gene } C_T - \text{GAPDH } C_T$) (27).

Western Blot Analysis

Frozen SCN tissue samples were homogenized by sonication in ice-cold extraction buffer (150 mM NaCl, 50 mM Tris HCl, 1 mM EDTA, 1% Triton X-100, 1% protease inhibitor cocktail; P8340, Sigma-Aldrich, St Louis, MO, USA) and the protein concentration was then determined by a Bio-Rad DC protein assay kit (500-0116, Bio-Rad, Hercules, CA, USA). The proteins (20 μg) were electrophoresed on a 7.5% acrylamide gel and then electrotransferred to a polyvinylidene difluoride (PVDF) membrane (GE Healthcare Biosciences, Piscataway, NJ, USA). Membranes were blocked for 1 h at room temperature with 5% non-fat milk in Tris-buffered saline containing 0.1% Tween 20 (TBST), and then incubated overnight at 4°C with a primary antibody against NCX2 (goat anti-NCX2, directed against a peptide sequence mapping within an extracellular domain of NCX2 of human origin; SC-33528; Santa Cruz, CA, USA) at 1:5,000 dilution (11, 44). After washing with TBST, membranes were processed with a horseradish peroxidase-conjugated anti-goat secondary antibody (1:5,000), and the protein bands were visualized using chemiluminescence (ECL reagent; GE Healthcare Biosciences). After detection of the

NCX2-immunoreactive bands, the same membranes were stripped and reprobed with a β-actin monoclonal antibody (1:20,000; A5441; Sigma-Aldrich) to confirm equal protein loading. For each sample, the optical density of the NCX2 band was quantified with ImageJ 1.45s (National Institutes of Health, Bethesda, MD, USA), normalized to the β-actin loading control, and then averaged across all gels.

Immunohistochemistry and Immunofluorescence

Sprague-Dawley rats (23–25 days old) were deeply anesthetized with Zoletil (40 mg/kg, i.p.; Virbac Laboratories, Carros, France) and fixed by transcardial perfusion with phosphate buffered saline (PBS) and then with 4% paraformaldehyde at 500 ml/animal. Brains were removed and post-fixed overnight for more than 16 h in 4% paraformaldehyde, followed by dehydration with 30% sucrose in PBS for another 24 h. Twenty micrometer-thick coronal sections through the hypothalamus region containing the SCN were cut on a cryostat chilled to –20°C, collected in an antifreeze solution, and stored in a –20°C freezer until further processing.

For immunohistochemical staining, 20 μm-sections were treated with 0.3% H₂O₂ for 15 min to quench endogenous peroxidase, and then incubated overnight at 4°C in PBS containing 2% serum, 0.3% Triton X-100, and primary antibodies against NCX2 (goat anti-NCX2; 1:200; SC-33528; Santa Cruz), VIP (rabbit anti-VIP; 1:3,000; ab43841; Abcam, Cambridge, MA, USA) (19), GRP (rabbit anti-GRP; 1:250; no. 250676; Abbiotec, CA, USA), and AVP (rabbit anti-AVP; 1:3,000; AB1565; Millipore) (8). Sections were then treated with respective biotinylated secondary antibodies for 1 h at room temperature. After rinsing in PBS, sections were incubated in avidin-biotin complex (ABC Elite Kit, Vector Labs, Burlingame, CA, USA) for 1 h according to the manufacturer's instructions. After two 10-min washes in 0.1 M sodium acetate, sections were stained with diaminobenzidine. Sections were photographed and analyzed with an inverted microscope integrated with the MT20 illumination system (Olympus Biosystems, Planegg, Germany).

For immunofluorescence staining, 20 μm-sections were washed for 20–30 min in PBS and then incubated overnight at 4°C in PBS containing 2% serum, 0.3% Triton X-100, and primary antibodies against NCX2 (goat anti-NCX2; 1:100; SC-33528; Santa Cruz), AVP (rabbit anti-AVP; 1:500; AB1565; Millipore), VIP (guinea pig anti-VIP; 1:500; T-5030; Peninsula Laboratories, San Carlos, CA, USA) (3), VIP (rabbit anti-VIP; 1:500; ab43841; Abcam), GRP (rabbit anti-GRP; 1:250; No. 250676; Abbiotec, CA, USA),

vesicular glutamate transporter type 2 (vGluT2) (guinea pig anti-vGluT2; 1:500; AB2251; Millipore, Temecula, CA, USA) (22), serotonin transporter (SERT) (rabbit anti-SERT; 1:500; AB9726; Millipore) (47), NPY (rabbit anti-NPY; 1:500; ab30914; Abcam) (29), Bassoon (mouse anti-Bassoon; 1:200; ADI-VAM-PS003-D; Enzo Life Sciences, Farmingdale, NY, USA) (7), and glial fibrillary acidic protein (GFAP) (rabbit anti-GFAP; 1:500; G9269; Sigma) (29). Sections were then treated with respective Alexa Fluor secondary antibodies 488, 568, or 633 (1:300; Molecular Probes, Eugene, OR, USA) and Hoechst 33342 (B-2261; Sigma) for 1 h at room temperature. After rinsing in PBS, sections were coverslipped with ProLong Gold anti-fade reagent (P36930; Molecular Probes) and photographed with a Zeiss LSM 510 confocal microscope. Contrast and brightness were optimized using Adobe Photoshop (Adobe Systems, San Jose, CA, USA).

Statistical Analysis

Data were analyzed with the commercial software GraphPad PRISM (GraphPad Software, San Diego, CA, USA). Data are presented as means \pm standard error of the mean (SEM) and were analyzed with analysis of variance (ANOVA), followed by *post hoc* Tukey's test. A *P*-value of 0.05 or less is considered statistically significant.

Results

Distribution Patterns of NCX2 and Neuropeptides AVP, VIP, and GRP in the Rat SCN

The distribution of immunoreactivity for NCX2 and three major neuropeptides AVP, VIP and GRP in mid-sections of the rat SCN (Fig. 1, encircled by dotted ovals) were performed with well-characterized antibodies against these antigens (Fig. 1). The NCX2 immunoreactivity was predominantly localized to the ventral region of the SCN (Fig. 1A; see also ref. 44), similar to the distribution pattern of VIP (Fig. 1B) and GRP (Fig. 1C), which receive photic glutamatergic inputs (32), but unlike the AVP immunoreactivity which was preferentially distributed to the dorsal region of the SCN (Fig. 1D).

The high magnification image revealed many large NCX2-immunoreactive puncta, \sim 1–2 μ m in size, scattering around and making appositions on the soma in the ventral region of the SCN (Fig. 1E). Furthermore, smaller NCX2-immunoreactive puncta were found around the circumference of a number of cells (Fig. 1E, marked by asterisks) and also in the perikarya of a few cells (Fig. 1E, inset). By contrast, in the dorsal region of the SCN, the NCX2-immunoreactive puncta

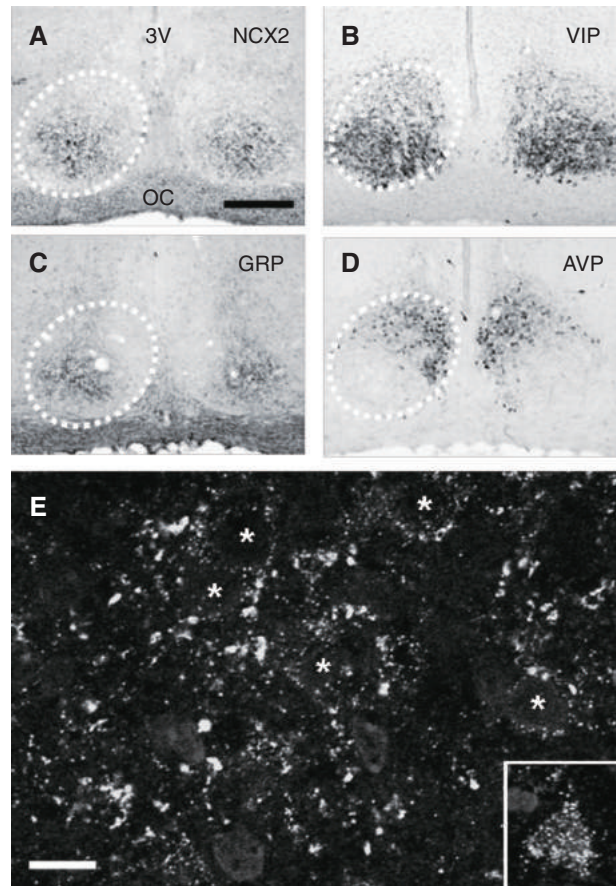


Fig. 1. Distribution patterns of NCX2, VIP, GRP and AVP immunoreactivity in the rat SCN. (A–D) Low-magnification images showing the distribution patterns of immunoreactivity for NCX2 (A), VIP (B), GRP (C) and AVP (D). Scale bar: 200 μ m. 3V: third ventricle. OC: optic chiasm. (E) High-magnification image showing the NCX2-immunoreactive puncta in the ventral SCN. Note the large NCX2-stained puncta often making appositions on cells, as indicated by Hoechst-stained nuclei in gray. Note also a number of cells having NCX2-immunoreactive puncta distributed around cell circumference, marked by asterisks. Inset: a cell stained with NCX2-immunoreactive puncta in the perikarya. Scale bar: 10 μ m.

were sparse in number and arranged themselves like a broken string of beads (data not shown).

Selective Colocalization of NCX2 with VIP, GRP and VIP/GRP

Double staining immunofluorescence for NCX2 and VIP (Fig. 2A), GRP (Fig. 2B), AVP (Fig. 2C), or the astroglial marker GFAP (not shown) were performed in the mid-SCN sections to determine the localization of NCX2 in specific types of cells. In agreement with similar distribution pattern of NCX2 and VIP or GRP, double labeling

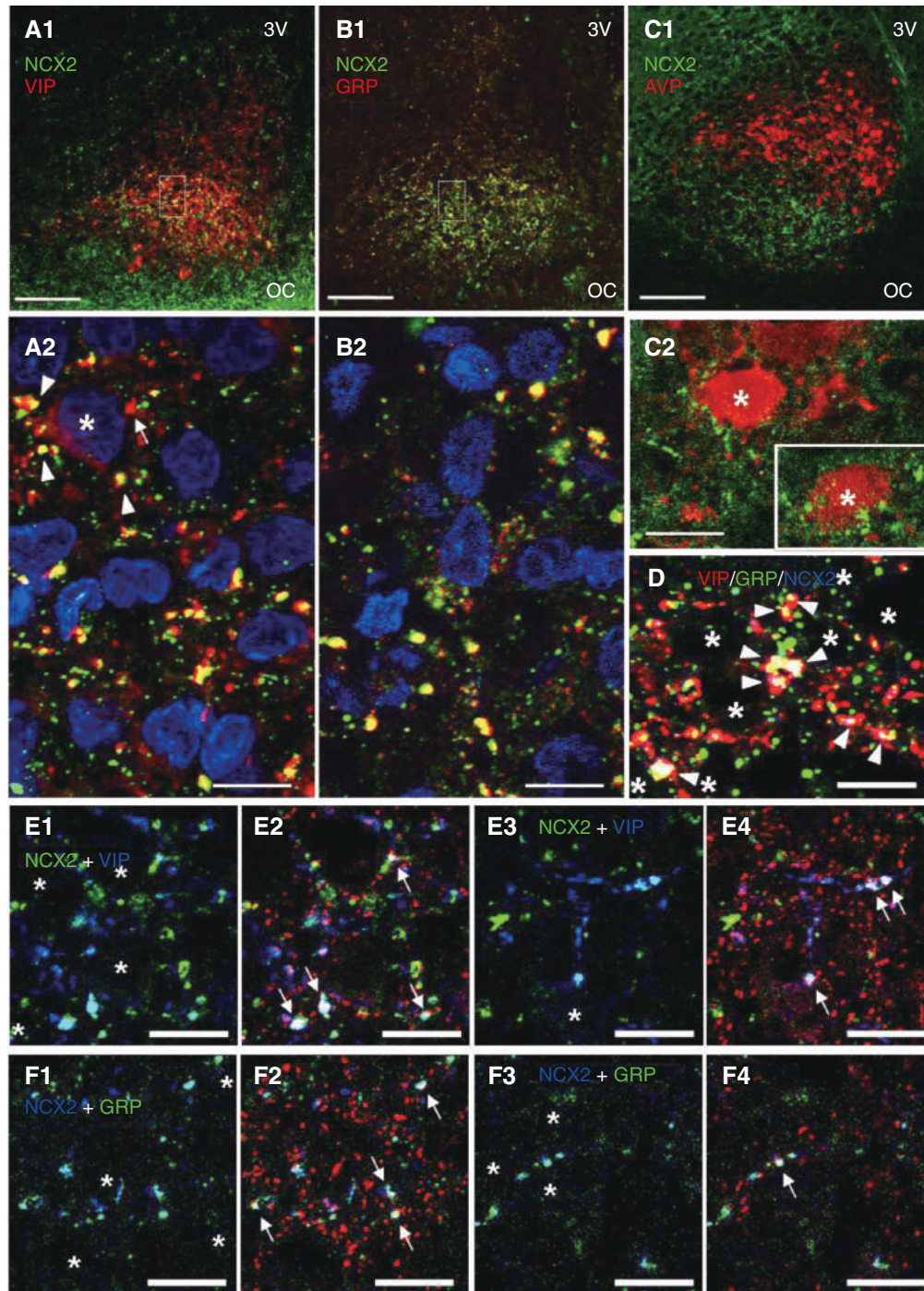


Fig. 2. Double and triple staining for NCX2, neuropeptides and Bassoon. (A–D) Selective colocalization of NCX2 with VIP, GRP, VIP/GRP, but not AVP. (A1, B1 & C1) Low magnification images showing the double staining patterns of NCX2 and VIP (A1), GRP (B1), or AVP (C1). (A2, B2 & C2) High magnification images showing colocalization of NCX2 and VIP (A2) or GRP (B2), as evidenced by the presence of yellow puncta, but not NCX2 and AVP (C2). Note the VIP-stained soma (marked with asterisk) surrounded by bouton-like puncta stained with NCX2/VIP (arrowheads) or VIP alone (arrow) (A2). Note also that the NCX2-immunoreactive boutons were in close apposition with AVP-stained somata (marked with asterisks) in the ventromedial SCN (C2). (D) Triple staining to demonstrate the colocalization of NCX2 with VIP/GRP (yellow). Note the VIP/GRP-immunoreactive puncta (yellow) in apposition with the soma (marked with asterisks), with many of the yellow puncta also co-stained with NCX2 (blue) to appear as white in color (arrowheads). 3V: third ventricle. OC: optic chiasm. Scale bar: 100 μ m (A1, B1 & C1); 10 μ m (A2, B2, C2, D1 & D2). (E and F) Presynaptic localization of Bassoon with NCX2/VIP and NCX2/GRP. (E1–E4) The colocalized NCX2 (green) and VIP (blue) in cyan puncta (E1, E3) mostly co-stained with Bassoon (red) to appear as white in color (E2 & E4, arrowheads). (F1–F4) A portion of colocalized NCX2 (blue) and GRP (green) in cyan puncta (F1, F3) also co-stained with Bassoon (red) to appear as white in color (F2 & F4, arrowheads). Scale bar: 10 μ m. Asterisks mark the Hoechst-stained nuclei.

indicated colocalization of NCX2 and VIP (Figs. 2A1 & 2A2) as well as NCX2 and GRP (Figs. 2B1 & 2B2). The double stains of NCX2/VIP (Fig. 2A2) or NCX2/GRP (Fig. 2B2) occurred often at large NCX2-immunoreactive puncta in apposition with the soma. Cells clearly stained with anti-VIP antibody (Fig. 2A2, asterisk) were also surrounded by bouton-like puncta stained with NCX2/VIP (Fig. 2A2, arrowheads) or VIP alone (Fig. 2A2, arrow). There was also intense colocalization between NCX2 and GRP as evidenced by the yellow color signifying double staining for both NCX2 (green) and GRP (red) (Fig. 2B1), with many of the GRP immunoreactive puncta also stained for NCX2 (Fig. 2B2).

In addition to the VIP and GRP cell groups, there is a third group of SCN neurons coexpressing VIP and GRP (2, 37, 39). Triple staining was thus used to determine whether the NCX2 immunoreactivity coexisted with VIP and GRP. An area where colocalization of VIP (red) and GRP (green) could be clearly visualized as yellow puncta surrounding or apposing the soma is shown in Fig. 2D, marked with asterisks. It was noted that many of these yellow puncta were also co-stained with the antibody for NCX2 (blue) to appear as white in color (Fig. 2D, arrowheads), indicating the localization of NCX2 in the VIP/GRP neurons.

In contrast to colocalization of NCX2 and VIP, GRP or VIP/GRP, no colocalization of NCX2 and AVP (Figs. 2C1, C2) or GFAP (not shown) was found. Instead, NCX2-immunoreactive bouton-like punctate stains could be found to be in close apposition with AVP-immunoreactive somata (Fig. 2C2, asterisks) located in the ventromedial region of the SCN.

Colocalization with the Presynaptic Marker Protein Bassoon

To further assess possible involvement of NCX2 in the regulation of VIP or GRP release, an antibody against the presynaptic cytomatrix protein Bassoon, a marker for presynaptic active zone (for review see ref. 10) and varicosity (20), was used to perform triple staining for Bassoon/NCX2/VIP (Figs. 2E1 to 2E4) and Bassoon/NCX2/GRP (Figs. 2F1 to 2F4). The results revealed that the colocalized VIP (blue) and NCX2 (green) in cyan puncta, surrounding or apposing the soma (Fig. 2E1), or in varicosity-like swelling along the process (Fig. 2E3), were mostly co-stained with the antibody for Bassoon (red) to appear as white in color (Figs. 2E2 & 2E4, arrowheads). Similarly, a portion of the colocalized GRP (green) and NCX2 (blue) in the cyan puncta (Figs. 2F1 & 2F3) was also co-stained with the anti-Bassoon antibody (red) to appear as white (Figs. 2F2 & 2F4, arrowheads). Taken together, the presence of triple stains for both Bassoon/NCX2/VIP

and Bassoon/NCX2/GRP indicates the localization of NCX2/VIP and NCX2/GRP at the presynaptic sites, suggesting that NCX2 may play a role in the regulation of VIP and GRP release.

Lack of Colocalization of NCX2 with Markers for Input Pathways

To determine the possible presence of NCX2 in afferent inputs to the SCN, antibodies for the vGluT2, SERT or NPY were used to perform double staining with NCX2 (Figs. 3A1, 3B1 & 3C1). The results indicated a lack of colocalization of NCX2 with any of the three markers for afferent inputs (Figs. 3A2, 3B2 & 3C2). Nevertheless, the NCX2-immunoreactive puncta (green) was in such close apposition with some of the SERT- or NPY-immunoreactive puncta (red) that the overlap of red and green puncta appeared as tiny yellow spots (Figs. 3B2 & 3C2).

Constancy in NCX2 Gene and Protein Expression

In vivo microdialysis experiments have previously revealed a circadian release of VIP and GRP from the SCN (13, 14). To investigate whether the NCX2 expression is rhythmic in the SCN, the mRNA and protein levels were measured at different time points by real-time PCR and western blot analysis, respectively (Fig. 4). The real-time PCR indicated a constancy in the NCX2 gene expression across the time points of the day tested ($P = 0.22$; $n = 4$ per time point, total $n = 32$) (Fig. 4A, left panel). In contrast, the clock genes *Per1* and *Per2* both exhibited a robust rhythmicity ($P < 0.001$), with the highest expression level at ZT 5 and the lowest at ZT 17 for *Per1* (Fig. 4A, middle panel), and ZT 8 and ZT 20 for *Per2* (Fig. 4A, right panel). The daily expression variations of *Per1* and *Per2* presented here are similar to those reported previously in the rat SCN (45).

Similar to a lack of daily variation in the gene expression, the western blot analysis also revealed no day-night variations in the NCX2 protein levels ($P = 0.38$) ($n = 4$ per time points, total $n = 16$; Fig. 4B). The results confirms our previous observation of constancy in the NCX2 immunoreactivity intensity between two time points at day (ZT 8) and at night time (ZT 14) (44). Taken together, the results indicate a lack of daily variation in the NCX2 gene expression and protein levels.

Discussion

The NCX plays an important role in the regulation of intracellular Ca^{2+} homeostasis by being able to extrude or uptake Ca^{2+} . The SCN expresses NCX1

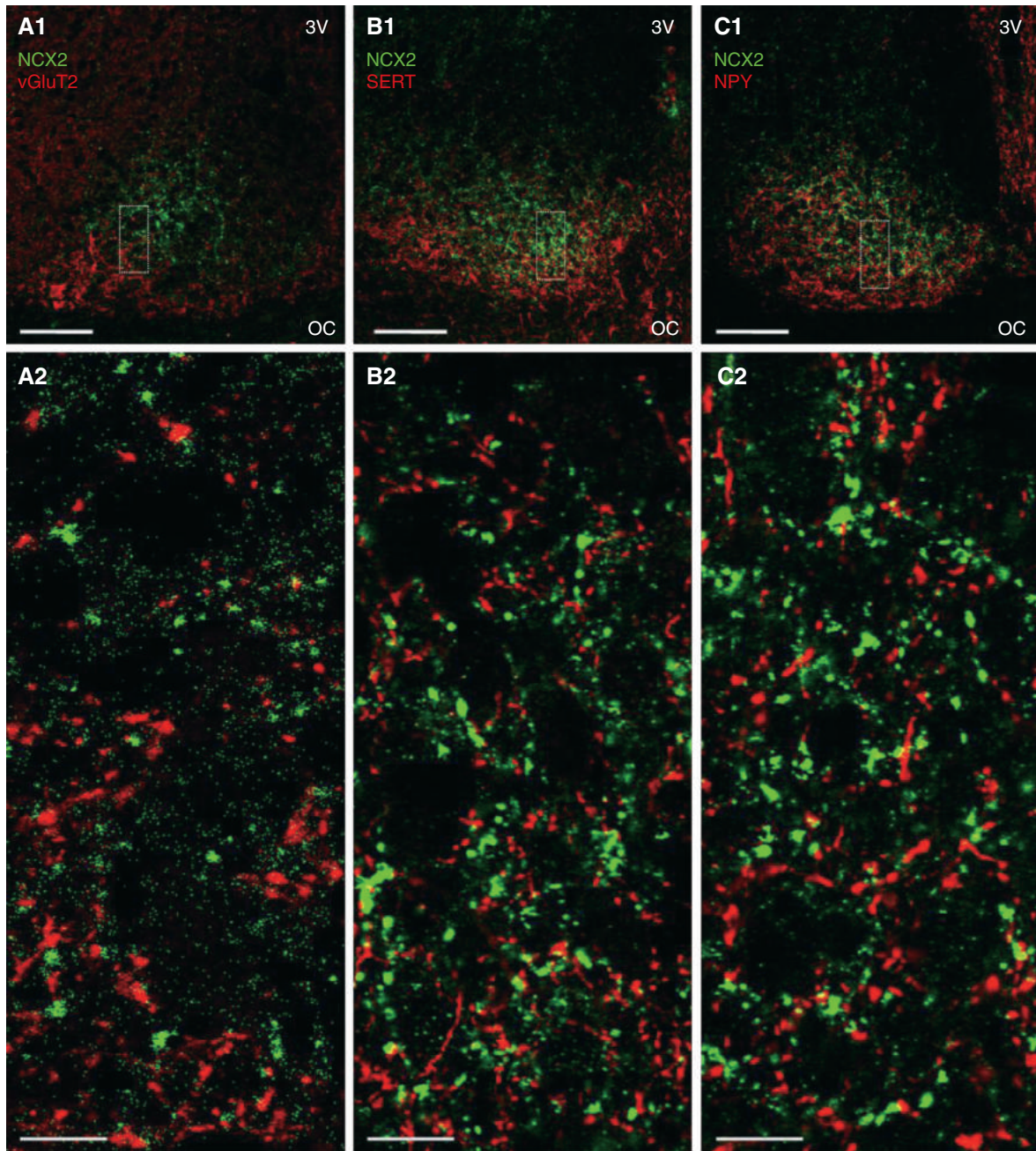


Fig. 3. Lack of colocalization of NCX2 with markers for three major afferent inputs. (A1, B1 & C1) Low magnification images showing the double staining patterns of NCX2 and vGluT2 (A1), SERT (B1), or NPY (C1). (A2, B2 & C2) High magnification images showing a lack of colocalization of NCX2 with vGluT2 (A2), SERT (B2) or NPY (C2). Note that the tiny yellow spots do not reflect true colocalization of NCX2 and SERT (B2) or NCX2 and NPY (C2), but are artifacts caused by overlap of red and green puncta due to close apposition. 3V: third ventricle. OC: optic chiasm. Scale bar: 100 μm (A1, B1, C1); 10 μm (A2, B2, C2).

and NCX2, with NCX1 distributed in the whole SCN but NCX2 restricted to the retinorecipient ventral SCN (44). We have previously used ratiometric Ca^{2+} imaging to demonstrate that NCX1 is responsible for rapid clearance of depolarization-induced Ca^{2+} influx in the SCN neurons (44). However, the role of NCX2 in the SCN remains unknown. This study determines

the colocalization of NCX2 with neuropeptides. Confirming our previous observation of restricted distribution of NCX2 in the ventral region of the SCN (44), the immunostaining results presented in this work showed a similar distribution pattern of NCX2 to those of VIP and GRP, both of which were expressed predominantly in the ventral SCN (32). Importantly,

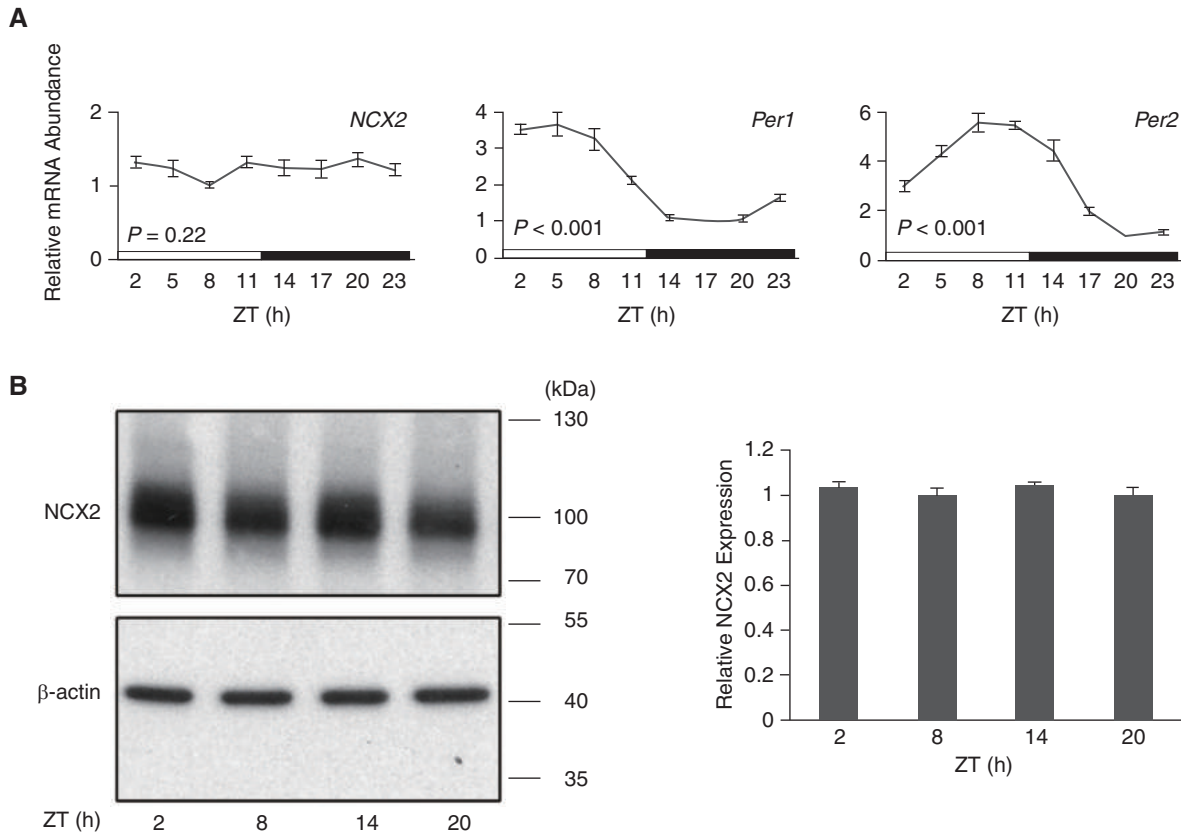


Fig. 4. Lack of circadian variation in NCX2 gene expression (A) and protein levels (B). (A) Real-time PCR results showing the daily mRNA profiles of NCX2 (left panel), *Per1* (middle panel) and *Per2* (right panel). White bars: light period; Black bars: dark period. (B) Western blot analysis showing the protein levels for NCX2 (102 kDa; left top panel) and β -actin (42 kDa; left bottom panel) at four different time points across the day. Right panel: statistics showing similar expression levels of NCX2 among different time points.

confocal images revealed colocalization of NCX2 with VIP, GRP and VIP/GRP in the ventral SCN, but not with AVP in the dorsal SCN region. NCX2 was found also not to colocalize with the astroglial marker GFAP or the markers for major input pathways, vGluT2, SERT, and NPY, to the retinorecipient ventral SCN. Together the results indicate a selective localization of NCX2 with VIP-, GRP- and VIP/GRP-expressing neurons.

Furthermore, the somata showing appositions of NCX2-, NCX2/VIP-, NCX2/GRP- or NCX2/VIP/GRP-immunoreactive boutons were also restricted to the ventral SCN, apparently due to the restricted distribution of NCX2 immunoreactivity in this region (Fig. 1). Presumably the cells receiving NCX2-immunoreactive boutons in the ventral SCN should include one of the three major cell groups, namely VIP, GRP and VIP/GRP neurons. Indeed, our results indicated that at least the VIP-immunoreactive soma appeared to be in apposition with both VIP- and NCX2/VIP-immunoreactive boutons. Interestingly, while NCX2 did not colocalize with AVP, the NCX2-immunoreactive bouton-like puncta could be found to extend to the

ventromedial area to be in close apposition with AVP neurons. Together the results suggest a rich innervation of NCX2-, NCX2/VIP-, NCX2/GRP- and NCX2/VIP/GRP-containing boutons on the cells in the ventral SCN, in line with reciprocal innervations between the VIP, GRP and VIP/GRP cell groups in the rat SCN (39).

In the rat SCN, putative peptidergic dense-core vesicles have been shown to be released from axonal terminals and somatodendritic areas of neurons with the tannic acid procedure (6); in cultured monkey GnRH-1 neurons, the presynaptic cytomatrix protein Bassoon has been shown to be associated with neuropeptide-containing large dense-core vesicles (15). We also performed in this work triple staining to determine the colocalization of Bassoon with NCX2/VIP or NCX2/GRP. Our result showed the presence of Bassoon/NCX2/VIP and Bassoon/NCX2/GRP triple-stained puncta in the varicosity-like swellings along the process and in bouton-like swellings making apposition on the soma, indicating the localization of NCX2/VIP and NCX2/GRP at the presynaptic sites (Fig. 2). It is not known, however, whether NCX2 may be associated with soluble N-ethylmaleimide-

sensitive factor activating protein receptor (SNARE) proteins and/or dense-core vesicles in the SCN. Nonetheless, other reported evidence has indicated that NCX2 colocalizes with the SNARE protein synaptosomal-associated protein 25 (SNAP-25) in synaptosomes prepared from the human cortex (42) and is associated with SNAP-25 within nanometers of voltage gated calcium channels 2 (CaV2) in the rat brain (34).

The demonstration of presynaptic localization of NCX2/VIP and NCX2/GRP suggests a possible involvement of NCX2 in the regulation of the release of VIP and GRP, most likely *via* way of clearing or uptaking Ca^{2+} at presynaptic release sites. We recently reported an important role of NCX1 in rapidly clearing depolarization-induced $[\text{Ca}^{2+}]_i$ increase in the soma of SCN neurons, as the inhibition of NCX slows the clearance of high K^+ -induced $[\text{Ca}^{2+}]_i$ increase (44). It is expected that NCX2 would play a similar role in clearing Ca^{2+} at presynaptic sites to regulate the release of VIP, GRP or VIP/GRP. Indeed, in the mouse hippocampal CA1 pyramidal neurons, NCX2 is the major protein for clearing Ca^{2+} at the presynaptic terminals, and in NCX2-knockout mice, the clearance of depolarization-induced $[\text{Ca}^{2+}]_i$ increase is markedly slowed down to enhance long-term potentiation (18). Nevertheless, since the NCX2-immunoreactive puncta were also be found around the circumference and/or in the perikarya of some cells in the ventral SCN in the present study (Fig. 1), it is possible that NCX2 may also play a role in the regulation of postsynaptic $[\text{Ca}^{2+}]_i$ in a small subset of SCN neurons.

In view of the observation that *in vivo* release of VIP and GRP from the hamster SCN is rhythmic (13, 14), we also investigated whether the NCX2 expression is rhythmic in the rat SCN. Our results revealed, however, a lack of daily variation in the NCX2 gene expression and protein levels, in sharp contrast to a robust circadian rhythm in the expression of clock genes *Per1* and *Per2* (Fig. 4), suggesting that other mechanisms, such as day-night variations in the firing rate and intracellular Ca^{2+} concentrations (9), may be involved in the circadian release of neuropeptides. Nevertheless, NCX2 activity is known to be stimulated by nitric oxide in a cyclic guanosine monophosphate (cGMP)-dependent manner, most likely mediated by acting on a segment of the intracellular f-loop with consensus phosphorylation site of cGMP-dependent protein kinase (PKG) (41). As the SCN exhibits a diurnal rhythm in cGMP levels, PKG and neuronal nitric oxide synthase activities (1, 12), it is possible that the NCX2 activity may change accordingly even with constant levels of expression.

In the SCN, VIP and GRP neurons directly receive

retinal input, responds to photic entrainment with light-induced *Per1/Per2* expression, and communicate phase-shifting events *via* way of VIP and GRP (for review see ref. 16). Although the application of VIP or GRP produces phase shifts of firing rhythm in SCN slices, only the light-responsive and *Per1*-inducible VIP neurons located in the ventrolateral SCN contain GRP (see ref. 21 and reference herein), suggesting that light-induced release of both VIP and GRP may have synergistic effects on phase shifting. In this context, our finding of selective colocalization of NCX2 with VIP, GRP and VIP/GRP may also suggest a NCX2 role in the regulation of photic entrainment.

Furthermore, in contrary to the restricted distribution of NCX2 to the ventral SCN, NCX1 is distributed in the whole SCN, albeit with more intense NCX1 immunoreactivity in the ventral than dorsal SCN (44). Although NCX1 is critically involved in postsynaptic Ca^{2+} clearing at least in the soma of SCN neurons (44), it may also regulate neuropeptide release. It would be interesting to know the colocalization of NCX1 with major neuropeptides such as VIP, GRP, and AVP. Furthermore, as the release of VIP, GRP and AVP from the SCN requires transmembrane Ca^{2+} influx (13, 14), the nature of Ca^{2+} sources, such as voltage-dependent Ca^{2+} channels, should also be an important issue for future studies. In this context, it is noteworthy that our unpublished observations from Ca^{2+} imaging and immunostaining experiments have indicated a functional interaction of NCX1 and CaV1.2 L-type Ca^{2+} channels in the regulation of depolarization-induced Ca^{2+} influx (manuscript in preparation).

In summary, we show here that NCX2 is selectively localized with VIP, GRP and VIP/GRP. The co-expression of Bassoon with NCX2/GRP and NCX2/VIP indicates their localization at presynaptic releasing sites, suggesting a NCX2 role in the regulation of release of GRP and VIP. We also show a lack of day-night variation in NCX2 mRNA and protein levels, in contrast to a robust circadian rhythm in the expression of clock genes *Per1* and *Per2*.

Conflict of Interest

The authors declared no conflicts of interest.

Acknowledgments

We are grateful to the Neuroscience Research Center, Chang Gung Memorial Hospital, Linkou, Taiwan. This work was supported by Chang Gung Medical Foundation (CMRPD1C0583 and CMRPD1F0111; R.C.H) and by Taiwan Ministry of Science and Technology (MOST103-2320-B-182-007; R.C.H).

References

- Agostino, P.V., Ferreyra, G.A., Murad, A.D., Watanabe, Y. and Golombek, D.A. Diurnal, circadian and photic regulation of calcium/calmodulin-dependent kinase II and neuronal nitric oxide synthase in the hamster suprachiasmatic nuclei. *Neurochem. Int.* 44: 617-625, 2004.
- Albers, H.E., Liou, S.Y., Stopa, E.G. and Zoeller, R.T. Interaction of colocalized neuropeptides: functional significance in the circadian timing system. *J. Neurosci.* 11: 846-851, 1991.
- Belenky, M.A., Yarom, Y. and Pickard, G.E. Heterogeneous expression of γ -aminobutyric acid and γ -aminobutyric acid-associated receptors and transporters in the rat suprachiasmatic nucleus. *J. Comp. Neurol.* 506: 708-732, 2008.
- Blaustein, M.P. and Lederer, W.J. Sodium/calcium exchange: its physiological implications. *Physiol. Rev.* 79: 763-854, 1999.
- Brown, T.M., Hughes, A.T. and Piggins, H.D. Gastrin-releasing peptide promotes suprachiasmatic nuclei cellular rhythmicity in the absence of vasoactive intestinal polypeptide-VPAC2 receptor signaling. *J. Neurosci.* 25: 11155-11164, 2005.
- Castel, M., Morris, J. and Belenky, M. Non-synaptic and dendritic exocytosis from dense-cored vesicles in the suprachiasmatic nucleus. *NeuroReport* 7: 543-547, 1996.
- Chen, J., Mizushige, T. and Nishimune, H. Active zone density is conserved during synaptic growth but impaired in aged mice. *J. Comp. Neurol.* 520: 434-452, 2011.
- Das, M., Vihlen, C.S. and Legradi, G. Hypothalamic and brainstem sources of pituitary adenylate cyclase-activating polypeptide nerve fibers innervating the hypothalamic paraventricular nucleus in the rat. *J. Comp. Neurol.* 500: 761-776, 2007.
- Dibner, C., Schibler, U. and Albrecht, U. The mammalian circadian timing system: organization and coordination of central and peripheral clocks. *Annu. Rev. Physiol.* 72: 517-549, 2010.
- Dresbach, T., Qualmann, B., Kessels, M.M., Garner, C.C. and Gundelfinger, E.D. The presynaptic cytomatrix of brain synapses. *Cell Mol. Life Sci.* 58: 94-116, 2001.
- Engelhardt, M., Vorwald, S., Sobotzik, J.M., Bennett, V. and Schultz, C. Ankyrin-B structurally defines terminal microdomains of peripheral somatosensory axons. *Brain Struct. Funct.* 218: 1005-1016, 2013.
- Ferreyra, G.A., Golombek, D.A. Rhythmicity of the cGMP-related signal transduction pathway in the mammalian circadian system. *Am. J. Physiol. Regul. Integr. Comp. Physiol.* 280: R1348-R1355, 2001.
- Francl, J.M., Kaur, G. and Glass, J.D. Regulation of VIP release in the SCN circadian clock. *NeuroReport* 21: 1055-1059, 2010.
- Francl, J.M., Kaur, G. and Glass, J.D. Roles of light and serotonin in the regulation of gastrin-releasing peptide and arginine vasopressin output in the hamster SCN circadian clock. *Eur. J. Neurosci.* 32: 1170-1179, 2010.
- Fuenzalida, L.C., Keen, K.L. and Terasawa, E. Colocalization of FM1-43, Bassoon, and GnRH-1: GnRH-1 release from cell bodies and their neuroprocesses. *Endocrinology* 152: 4310-4321, 2011.
- Golombek, D.A. and Rosenstein, R.E. Physiology of circadian entrainment. *Physiol. Rev.* 90: 1063-1102, 2010.
- Iwamoto, T. and Shigekawa, M. Differential inhibition of $\text{Na}^+/\text{Ca}^{2+}$ exchanger isoforms by divalent cations and isothiourea derivative. *Am. J. Physiol. Cell Physiol.* 275: C423-C430, 1998.
- Jeon, D., Yang, Y.M., Jeong, M.J., Philipson, K.D., Rhim, H. and Shin, H.S. Enhanced learning and memory in mice lacking $\text{Na}^+/\text{Ca}^{2+}$ exchanger 2. *Neuron* 38: 965-976, 2003.
- Jones, J.R., Tackenberg, M.C. and McMahon, D.G. Manipulating circadian clock neuron firing rate resets molecular circadian rhythms and behavior. *Nat. Neurosci.* 18: 373-375, 2015.
- Juranek, J., Mukherjee, K., Rickmann, M., Martens, H., Calka, J., Sudhof, T.C. and Jahn, R. Differential expression of active zone proteins in neuromuscular junctions suggests functional diversification. *Eur. J. Neurosci.* 24: 3043-3052, 2006.
- Kawamoto, K., Nagano, M., Kanda, F., Chihara, K., Shigeyoshi, Y. and Okamura, H. Two types of VIP neuronal components in rat suprachiasmatic nucleus. *J. Neurosci. Res.* 74: 852-857, 2003.
- Kiss, J., Csáki, Á., Csaba, Z. and Halász, B. Synaptic contacts of vesicular glutamate transporter 2 fibres on chemically identified neurons of the hypothalamic suprachiasmatic nucleus of the rat. *Eur. J. Neurosci.* 28: 1760-1774, 2008.
- Leak, R.K., Card, J.P. and Moore, R.Y. Suprachiasmatic pacemaker organization analyzed by viral transynaptic transport. *Brain Res.* 819: 23-32, 1999.
- Lee, S.L., Yu, A.S. and Lytton, J. Tissue-specific expression of $\text{Na}^+/\text{Ca}^{2+}$ exchanger isoforms. *J. Biol. Chem.* 269: 14849-14852, 1994.
- Li, Z., Matsuoka, S., Hryshko, L.V., Nicoll, D.A., Bersohn, M.M., Burke, E.P., Lifton, R.P. and Philipson, K.D. Cloning of NCX2 isoform of the plasma membrane $\text{Na}^+/\text{Ca}^{2+}$ exchanger. *J. Biol. Chem.* 269: 17434-17439, 1994.
- Linck, B., Qiu, Z.Y., He, Z.P., Tong, Q.S., Hilgemann, D.W. and Philipson, K.D. Functional comparison of the three isoforms of the $\text{Na}^+/\text{Ca}^{2+}$ exchanger (NCX1, NCX2, NCX3). *Am. J. Physiol. Cell Physiol.* 274: C415-C423, 1998.
- Livak, K.J. and Schmittgen, T.D. Analysis of relative gene expression data using real-time quantitative PCR and the $2^{-\Delta\Delta C_T}$ method. *Methods* 25: 402-408, 2001.
- Maywood, E.S., Reddy, A.B., Wong, G.K., O'Neill, J.S., O'Brien, J.A., McMahon, D.G., Harmar, A.J., Okamura, H. and Hastings, M.H. Synchronization and maintenance of timekeeping in suprachiasmatic circadian clock cells by neuropeptidergic signaling. *Curr. Biol.* 16: 599-605, 2006.
- Marx, M., Haas, C.A. and Haussler, U. Differential vulnerability of interneurons in the epileptic hippocampus. *Front. Cell Neurosci.* 7: 167, 2013.
- Meijer, J.H. and Schwartz, W.J. In search of the pathways for light-induced pacemaker resetting in the suprachiasmatic nucleus. *J. Biol. Rhythms* 18: 235-249, 2003.
- Molinaro, P., Viggiano, D., Nistico, R., Sirabella, R., Secondo, A., Boscia, F., Pannaccione, A., Scorziello, A., Mehdaoui, B., Sokolow, S., Herchuelz, A., Di Renzo G.F. and Annunziato, L. $\text{Na}^+/\text{Ca}^{2+}$ exchanger (NCX3) knock-out mice display an impairment in hippocampal long-term potentiation and spatial learning and memory. *J. Neurosci.* 31: 7312-7321, 2011.
- Moore, R.Y., Speh, J.C. and Leak, R.K. Suprachiasmatic nucleus organization. *Cell Tissue Res.* 309: 89-98, 2002.
- Morin, L.P. and Allen, C.N. The circadian visual system, 2005. *Brain Res. Rev.* 51: 1-60, 2006.
- Müller, C.S., Haupt, A., Bildl, W., Schindler, J., Knaus, H.G., Meissner, M., Rammner, B., Striessnig, J., Flockerzi, V., Fakler, B. and Schulte, U. Quantitative proteomics of the Cav2 channel nano-environments in the mammalian brain. *Proc. Natl. Acad. Sci. USA* 107: 14950-14957, 2010.
- Nicoll, D.A., Longoni, S. and Philipson, K.D. Molecular cloning and functional expression of the cardiac sarcolemmal $\text{Na}^+/\text{Ca}^{2+}$ exchanger. *Science* 250: 562-565, 1990.
- Nicoll, D.A., Quedneau, B.D., Qui, Z., Xia, Y.R., Lusic, A.J. and Philipson, K.D. Cloning of a third mammalian $\text{Na}^+/\text{Ca}^{2+}$ exchanger, NCX3. *J. Biol. Chem.* 271: 24914-24921, 1996.
- Okamura, H., Murakami, S., Uda, K., Sugano, T., Takahashi, Y., Yanaihara, C., Yanaihara, N. and Ibata, Y. Coexistence of vasoactive intestinal peptide (VIP)-, peptide histidine isoleucine amide (PHI)-, and gastrin-releasing peptide (GRP)-like immunoreactivity in neurons of the rat suprachiasmatic nucleus. *Biomed. Res.* 7: 295-299, 1986.
- Papa, M., Canitano, A., Boscia, F., Castaldo, P., Sellitti, S., Porzig, H., Tagliabattola, M. and Annunziato, L. Differential expression

- of the $\text{Na}^+\text{-Ca}^{2+}$ exchanger transcripts and proteins in rat brain regions. *J. Comp. Neurol.* 461: 31-48, 2003.
39. Romijn, H.J., Sluiter, A.A., Pool, C.W., Wortel, J. and Buijs, R.M. Evidence from confocal fluorescence microscopy for a dense, reciprocal innervation between AVP-, somatostatin-, VIP/PHI-, GRP-, and VIP/PHI/GRP-immunoreactive neurons in the rat suprachiasmatic nucleus. *Eur. J. Neurosci.* 9: 2613-2623, 1997.
 40. Sharma, V. and O'Halloran, D.M. Recent structural and functional insights into the family of sodium calcium exchangers. *Genesis* 52: 93-109, 2014.
 41. Secondo, A., Molinaro, P., Pannaccione, A., Esposito, A., Cantile, M., Lippiello, P., Sirabella, R., Iwamoto, T., Di Renzo, G. and Annunziato, L. Nitric oxide stimulates NCX1 and NCX2 but inhibits NCX3 isoform by three distinct molecular determinants. *Mol. Pharmacol.* 79: 558-568, 2011.
 42. Sokolow, S., Luu, S.H., Headley, A.J., Hanson, A.Y., Kim, T., Miller, C.A., Vinters, H.V. and Gyls, K.H. High levels of synaptosomal $\text{Na}^+\text{-Ca}^{2+}$ exchangers (NCX1, NCX2, NCX3) co-localized with amyloid-beta in human cerebral cortex affected by Alzheimer's disease. *Cell Calcium* 49: 208-216, 2011.
 43. Thurneysen, T., Nicoll, D.A., Philipson, K.D. and Porzig, H. Sodium/calcium exchanger subtypes NCX1, NCX2 and NCX3 show cell-specific expression in rat hippocampus cultures. *Mol. Brain Res.* 197: 145-156, 2002.
 44. Wang, Y.C., Chen, Y.S., Cheng, R.C. and Huang, R.C. Role of $\text{Na}^+\text{-Ca}^{2+}$ exchanger in Ca^{2+} homeostasis in the rat suprachiasmatic nucleus neurons. *J. Neurophysiol.* 113: 2114-2126, 2015.
 45. Yan, L., Takekida, S., Shigeyoshi, Y. and Okamura, H. *Per1* and *Per2* gene expression in the rat suprachiasmatic nucleus: circadian profile and the compartment-specific response to light. *Neuroscience* 94: 141-150, 1999.
 46. Yu, L. and Colvin, R.A. Regional differences in expression of transcripts for $\text{Na}^+\text{-Ca}^{2+}$ exchanger isoforms in rat brain. *Brain Res. Mol. Brain Res.* 50: 285-292, 1997.
 47. Zhou, F.C., Xu, Y., Bledsoe, S., Lin, R. and Kelley, M.R. Serotonin transporter antibodies: production, characterization, and localization in the brain. *Brain Res. Mol. Brain Res.* 43: 267-278, 1996.